

# A numerical approach to the voltammograms of a thick plate Pd|H electrode

Wu-Shou Zhang<sup>a,b,c,\*</sup>, Xin-Wei Zhang<sup>b</sup>

<sup>a</sup> Institute of Physics and Center for Condensed Matter Physics, Chinese Academy of Sciences, P.O. Box 603-99, Beijing 100080, People's Republic of China

<sup>b</sup> Institute of Applied Physics and Computational Mathematics, P.O. Box 8009, Beijing 100088, People's Republic of China

<sup>c</sup> Institute of Theoretical Physics, Shanxi University, Taiyuan 030006, People's Republic of China

Received 14 April 1997; received in revised form 13 October 1997

## Abstract

The kinetics of H sorption in a thick plate Pd|H electrode in cyclic voltammetry (CV) are studied by numerical methods and the effects of various parameters on the peak potential, peak current and hydrogen concentration are discussed. We find that the hydrogen concentration in PdH<sub>x</sub> is much less than the equilibrium value and give a simple criterion for the existence of phases occurring during CV. The voltammetric electro-sorption of H into Pd and electro-desorption of H from Pd are controlled by the adsorption of H on Pd and diffusion of H in Pd, respectively. By comparison with the previous experimental results, it is concluded that there are two sorts of adsorption, strong and weak playing key roles in H absorption into Pd at anodic and cathodic overpotentials (vs. RHE), respectively. © 1998 Elsevier Science S.A. All rights reserved.

**Keywords:** Cold fusion; Cyclic voltammetry; Kinetics; Pd|H electrode; Pd|H system

## 1. Introduction

In an earlier paper [1], we presented a model describing the quantity of H(D) absorbed into a Pd cathode under steady state conditions in the hydrogen evolution reaction (her). But for a practical Pd|H<sub>2</sub>O electrochemical system, the dynamic behaviour is a technologically important issue. For example, in the research and development of the Pd–H battery and other sorts of M–H battery, the charge-discharge characteristics are the key factors [2–4]. In cold fusion experiments, there is ample evidence to indicate that one essential condition for reproducibility of the excess heat is the existence of a deuterium (hydrogen) current [5,6], in other words, cold fusion arises from kinetics but not thermodynamics of the Pd|H(D) system.

Since the announcement of cold fusion [7], many theorists have focused their efforts on the kinetics of the Pd|H(D) electrode [2,3,8–15]. Most of the work was concerned with the charging and/or discharging process [2,3,8–11] or electrochemical impedance spectroscopy [12–15]. On the other hand, there were many experiments on cyclic voltammetry (CV) of the Pd|H electrode [16–23], but no theory was available. In this paper, we will discuss the kinetics of formation of the Pd|H (including Pd|D, the same below) electrode in CV.

## 2. Model

Unlike other metal|H electrodes, processes in the Pd|H electrode involve bulk Pd–H interactions such as H absorption and diffusion etc. Besides the Volmer, Tafel, Heyrovsky and penetration reactions mentioned in the earlier paper [1], we consider the H diffusion in bulk Pd

\* Corresponding author. E-mail: wszhang@aphy01.iphy.ac.cn

$$\Gamma_b F \frac{\partial x}{\partial t} = -\nabla \cdot j_d \quad (1)$$

$$j_d = -D\Gamma_b F \nabla x \quad (2)$$

where  $x$  is the relative concentration of H, i.e. the atom ratio of H to Pd, at a point in bulk Pd;  $j_d$  is the diffusion current density (cd) at the same place;  $\Gamma_b = 0.113 \text{ mol cm}^{-3}$  is the maximum molar number of available sites for H per unit volume; and  $D$  is the diffusion coefficient of H in Pd.

Consider an infinite Pd plate immersed in a pool of electrolyte, provided that  $D$  is independent of  $x$ , we have

$$\frac{\partial x}{\partial t} = D \frac{\partial^2 x}{\partial^2 y} \quad (3)$$

along the thickness direction of the Pd plate, where  $y$  is the distance measured from the outer Pd surface. The boundary conditions at the outer and inner surfaces are

$$j_d = -j_p, \quad y = 0 \quad (4)$$

$$j_d = -D\Gamma_b F \frac{\partial x}{\partial y} = 0 \quad y = d \quad (5)$$

where  $j_p$  is the current density of the penetration reaction [1], and  $d$  is the thickness of the Pd plate (for one side exposed to the electrolyte and the other side in contact with a hydrogen-impermeable substrate) or a half of the thickness (for both sides exposed to the electrolyte). Eq. (4) establishes a relation between the surface and bulk processes; it means that H atoms penetrating from the outer surface to the subsurface will diffuse into the depth of the bulk Pd. Eq. (5) is the condition of zero flux.

Combining Eqs. 1–6 in Ref. [1] and Eqs. (1)–(5) in the present paper, we establish a model of kinetics for a single metal hydride phase of Pd|H electrode.

In contrast to the earlier paper, we discuss only the case of potentials positive to the her. The Heyrovsky step and Tafel reaction are omitted because the former exists only at high cathodic overpotential in the her and the latter is limited by the  $\text{H}_2$  dissolution and diffusion in the electrolyte. We do not consider the capacity current either because it can be assumed as a constant in a half period of CV. So Eqs. 5 and 6 in Ref. [1] are simplified to

$$r\Gamma_s F \frac{d\theta}{dt} = j_p - j_v \quad (6)$$

$$j = j_v \quad (7)$$

where  $r$  is the roughness factor;  $\Gamma_s$  is the maximum molar number of available sites for H on real unit area [1], we choose the Pd(100) as the standard real surface on which  $\Gamma_s = 2.197 \times 10^{-9} \text{ mol cm}^{-2}$  [23];  $\theta$

is the relative surface coverage of H on Pd;  $j_v$  is the current density of the Volmer step. In order to be consistent with convention, we use  $E$  (vs. RHE) to replace  $\eta$  in Ref. [1] as the overpotential.

The parameters of CV are defined as:  $T$  is the period of CV;  $v = |dE/dt|$ , is the potential sweep rate;  $E_a$  ( $E_c$ ) is the upper (lower) potential limit;  $j_{ma}$  is the peak value of cd in the positive scan;  $E_{ma}$  is the potential corresponding to  $j_{ma}$ .

In this paper, we call the back processes of adsorption and absorption as de-adsorption and desorption respectively, this is different from the traditional usage in which desorption is regarded as both the back processes of adsorption and absorption equally.

Besides the simplifications mentioned above, our treatment is confined to the three points below:

1. The exchange cd of the penetration reaction,  $j_{op}$ , is so large that the penetration reaction is under a pseudoequilibrium.
2. We are concerned only with the situation of a single solid solution phase of  $\text{PdH}_x$ , i.e. the  $\alpha$ -phase.
3. The thickness of the Pd plate is much greater than the diffusion distance in one CV period, i.e.  $d^2 \gg \pi DT$ . Other cases, the surface Pd|H electrode ( $d=0$ ) and thin layer Pd|H electrode ( $d \ll \pi DT$ ), can be described in terms of the adsorption of H on metal [23–25] which has been studied extensively [26–29], so we do not discuss them again.

Eqs. 1 and 4 in Ref. [1] and Eqs. (1)–(7) in the present paper form a set of stiff partial differential equations that can be solved using, e.g. the Treanor method. The initial values are chosen for convenience as the stable CV result is independent of them.

### 3. Results

Prior to detailed discussion, we estimate the relaxation time  $\tau$  for stabilising a voltammogram. Provided that the Volmer step is the rate determining step (rds) in the initial cycles of CV, we have

$$\tau \sim d\Gamma_b F x_0 / (rj_{ov}) \quad (8)$$

where  $x_0$  is the equilibrium loading ratio of H in  $\alpha$ -PdH<sub>x</sub>,  $j_{ov}$  is the exchange current density of the Volmer step. Choosing  $d = 0.05 \text{ cm}$ ,  $x_0 = 0.1$  and  $r = 2$ ,  $j_{ov} = 0.5 \text{ mA cm}^{-2}$ , we obtain  $\tau \sim 7.9 \times 10^3 \text{ s} = 2.2 \text{ h}$ ; this is a very long time as observed in experiments [21].

For a practical Pd|H electrode, a stable CV result must be subject to the boundary conditions at the inner and outer surfaces, and periodicity of all the physical quantities. On the other hand, all processes of surface and bulk must be at equivalent rates, so the voltammogram contains characters of both of them; we first describe it by the former.

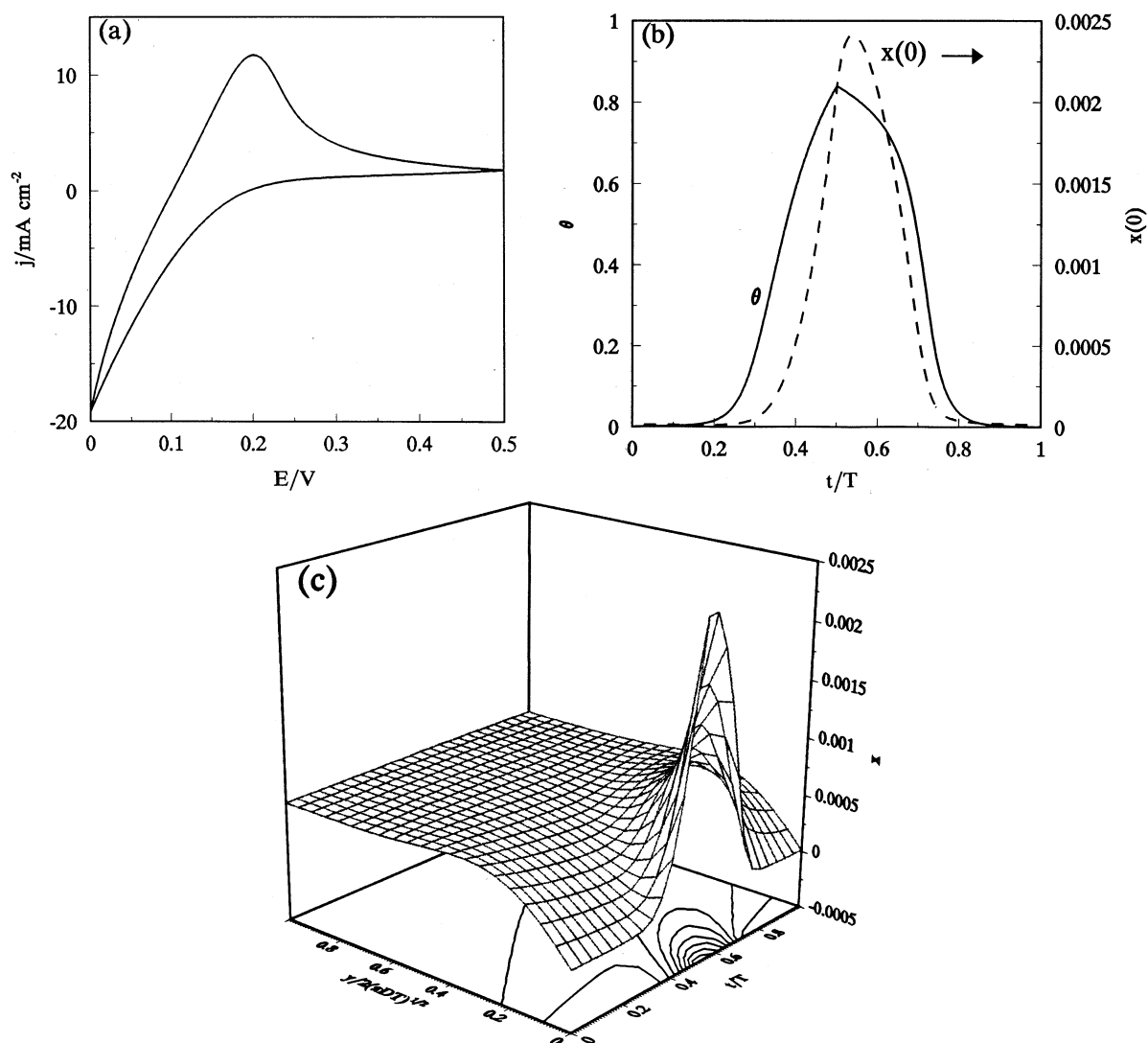


Fig. 1. An example of CV results of the thick plate Pd|H electrode. (a) The voltammogram, (b) the relative surface coverage of H,  $\theta$ , and the subsurface concentration of H,  $x(0)$ , as functions of time  $t/T$ , (c) the H distribution as a function of time. Parameters:  $j_{0V} = 0.5 \text{ mA cm}^{-2}$ ,  $\theta_0 = 0.99$ ,  $r = 2$ ,  $u = 2$ ,  $v = 0.1 \text{ V s}^{-1}$ ,  $j_{0P} = 50 \text{ mA cm}^{-2}$ ,  $x_0 = 0.1$ ,  $u_b = 0$ ,  $d = 2(\pi DT)^{1/2}$ ,  $D = 3.8 \times 10^{-7} \text{ cm}^2 \text{ s}^{-1}$ .  $t/T = 0-0.5$  is for the negative scan and  $t/T = 0.5-1$  is for the positive scan.

### 3.1. Adsorption characteristics of the voltammograms

For the rds being the Volmer step and referring to Eq. 1 in Ref. [1] (heterogeneity factor,  $u = 0$ ) and Eq. (7), we obtain

$$j = j_{*V} \left\{ \frac{\theta_*}{\theta_0} \exp \left[ \frac{1}{2} f(E - E_*) \right] - \frac{1 - \theta}{1 - \theta_*} \exp \left[ -\frac{1}{2} f(E - E_*) \right] \right\} \quad (9)$$

with

$$\frac{j_{*V}}{rj_{0V}} = \frac{\theta_*}{\theta_0} \exp \left[ \frac{1}{2} fE_* \right] = \frac{1 - \theta_*}{1 - \theta_0} \exp \left[ \frac{1}{2} fE_* \right] = g^{1/2}(\theta_*) \quad (10)$$

$$g(\theta) = \frac{\theta(1 - \theta)}{\theta_0(1 - \theta_0)} \quad (11)$$

where  $\theta_*$  ( $E_*$ ) is the value of  $\theta(E)$  at  $j = 0$  in the positive scan and  $\theta_0$  is the equilibrium value of  $\theta$ . Under extremely irreversible conditions,  $\theta$  and  $\theta_* \ll 1$ , we have

$$j = j_{*V} \left\{ \frac{\theta}{\theta_*} \exp \left[ \frac{1}{2} f(E - E_*) \right] - \exp \left[ -\frac{1}{2} f(E - E_*) \right] \right\} \quad (12)$$

It is easy to reveal some properties of the voltammograms from this equation. When  $E$  is close to  $E_*$ , the polarization is linear, i.e.  $j \sim E$  is a linear function (see Fig. 1(a)); when  $f(E - E_*) < -1$ , the cd is dominated by the cathodic component and it is controlled by  $E$  but is independent of  $\theta$ ; this means that the cd in the

positive and negative scans are close (even coincide) to each other as seen in many experiments [16–23]; when  $f(E - E_*) > 1$ , both terms  $\theta/\theta_*$  and  $\exp(f(E - E_*)/2)$  contribute to the cd. Thus, there are two situations: when  $E_a < E_{ma}$ , the term  $\exp(f(E - E_*)/2)$  dominates the cd and the voltammograms of the positive and negative scan are close to each other; otherwise, the cd is controlled by the term  $\theta/\theta_*$  and the voltammograms of different scan directions depart from each other (see Fig. 1(a)).

The different influences of  $\theta$  and  $E$  originate from the fact that  $\theta$  is an integral function of time (proportional to  $E$ ), so  $\theta$  is affected by the history of process and it has different effects at different scan directions.

The quantity  $E_*$  in Eqs. (9) and (10) is an indication of the phase state of PdH<sub>x</sub> in CV. This is because  $E_*$  corresponds to the turning point from desorption to absorption, i.e. the subsurface H concentration  $x(0)$  reaches its maximum value (maximum chemical potential correspondingly, see Fig. 1(c)), so  $E_*$  can be used as a criterion by comparison with  $E_{\beta\alpha}$ , the potential in the  $\beta \rightarrow \alpha$ -phase transition during desorption of hydrogen. If  $E_* > E_{\beta\alpha}$  ( $x(0) < x_\alpha$ , the maximum  $x$  in  $\alpha$ -PdH<sub>x</sub>) the overall process is confined to the  $\alpha$ -phase, otherwise, the  $\beta$ -phase is reached. For example,  $E_* = 0.103$  V and  $E_* > E_{\beta\alpha} \approx 0.06$  V [30] in Fig. 1(a), this means that Fig. 1(a) represents a voltammogram of PdH<sub>x</sub> with the  $\alpha$ -phase alone as indicated in Fig. 1(c).

### 3.2. Diffusion characteristics of the voltammograms

We notice that H atoms in bulk Pd behave to some extent like electro-active substances in solutions in CV. There is a plateau distribution of H concentration in  $y > (\pi DT)^{1/2}$  as shown in Fig. 1(c), the constant H concentration  $\Gamma_b x_{0,CV}$  is equivalent to the bulk concentration  $c_o^*$  in diffusion CV experiments [31].

Although  $x_{0,CV}$  does not change in one period in a stable CV, it can be altered by various parameters as shown in Fig. 2. This is an important distinction between the Pd–H system and the classical diffusion system in CV experiments. The reason is that the practical Pd|H electrode is a finite size other than an infinite size system so its behaviour is determined by external conditions, and given conclusions for classical diffusion systems cannot be applied directly. In this case,  $x_{0,CV}$  can be obtained only by numerical calculation. Because of its properties of finite size, the total charge involved in one period,  $\oint j dt = 0$  for a stable CV. If this condition is not fulfilled, it means that the voltammogram is unstable.

Due to the high irreversibility of H absorption into the thick Pd plate, we observe only the peak of the positive scan in the voltammograms. So we can refer the results of linear sweep voltammetry (LSV). For a totally irreversible reaction, referring to Eq. (6.3.7) in Ref. [31] and replacing  $c_o^*$  by  $\Gamma_b x_{0,CV}$ , we obtain the desorption cd

$$j = \Gamma_b F x_{0,CV} \sqrt{\frac{1}{2} \pi D f v} \chi\left(\frac{1}{2} f E\right) \quad (13)$$

where  $\chi(fE/2)$  is the current function for irreversible charge transfer [31]; the maximum value is 0.2797. Choosing the parameters in Fig. 1 as an example:  $x_{0,CV} = 5.4 \times 10^{-4}$ ,  $D = 3.8 \times 10^{-7}$  cm<sup>2</sup> s<sup>-1</sup>,  $v = 0.1$  V s<sup>-1</sup>, we obtain the coefficient ahead of  $\chi(fE/2)$  as 9 mA cm<sup>-2</sup>. The peak cd correspondingly is 2.5 mA cm<sup>-2</sup> which is smaller than the numerical value, 11.7 mA cm<sup>-2</sup>; the reason for the discrepancy is that the peak potential shifts to a higher value as discussed below.

Analogously to Eq. (6.3.12) in Ref. [31], we obtain the peak potential associated with Eq. (13)

$$E_{ma} = \frac{2}{f} \left\{ 0.780 + \ln\left(\frac{\Gamma_b F x_0}{r j_{ov}}\right) + \frac{1}{2} \ln\left(\frac{1}{2} D f v\right) \right\} \quad (14)$$

Choosing  $x_0 = 0.1$  and other parameters as above, we obtain  $E_{ma} = 0.39$  V. Due to the high irreversibility and the finite size properties of the system, the peak potential in CV, 0.2 V is lower than that in LSV as shown in Fig. 1(a). We will see below that this formula describes the changes of  $E_{ma}$  with related parameters very well.

As discussed above, the emergence of the cd peak is caused by the dilution of H in the vicinity of the outer surface. When the peak is passed, the cd is maintained by diffusion of H atoms from the depth of the Pd plate and we obtain the cd expression analogous to that in a potential step transient experiment

$$j = \Gamma_b F D \frac{x_{0,CV}}{\sqrt{\pi D t}} \quad (15)$$

where time  $t$  is counted from a potential  $E_0$  which is about  $E_{ma}$ . Choosing  $x_{0,CV} = 5.4 \times 10^{-4}$ ,  $v = 0.1$  V s<sup>-1</sup>,  $E_0 = 0.3$  V,  $E = 0.5$  V, we obtain  $j = 1.3$  mA cm<sup>-2</sup> which is consistent with the numerical result, 1.7 mA cm<sup>-2</sup> in Fig. 1(a). This relation is valid covering the range of the rest of positive scan and part of the negative scan till the onset of H absorption.

From Fig. 1(c), we find  $x$  does not change in the range  $y > (\pi DT)^{1/2}$ . This means our treatment can be applied not only to the plate Pd but also to Pd wires or Pd spheres when their radii are much greater than  $(\pi DT)^{1/2}$ .

Fig. 2. Effects of different parameters on the characteristic quantities,  $E_{ma}$  (—),  $j_{ma}$  (•••) and  $x_{0,CV}$  (-•-) in CV. (a) Effects of  $j_{ov}$ , (b) effects of  $\theta_0$ , (c) effects of  $x_0$ , (d) effects of  $D$ , (e) effects of  $v$ , (f) effects of  $E_c$ . All the parameters are the same as those of Fig. 1 except for the independent variables in each figures and  $E_{ma}$  which is 0.9, 0.6, 0.7, 0.5, 0.5 and 0.5 for the figures in alphabetical order, respectively.

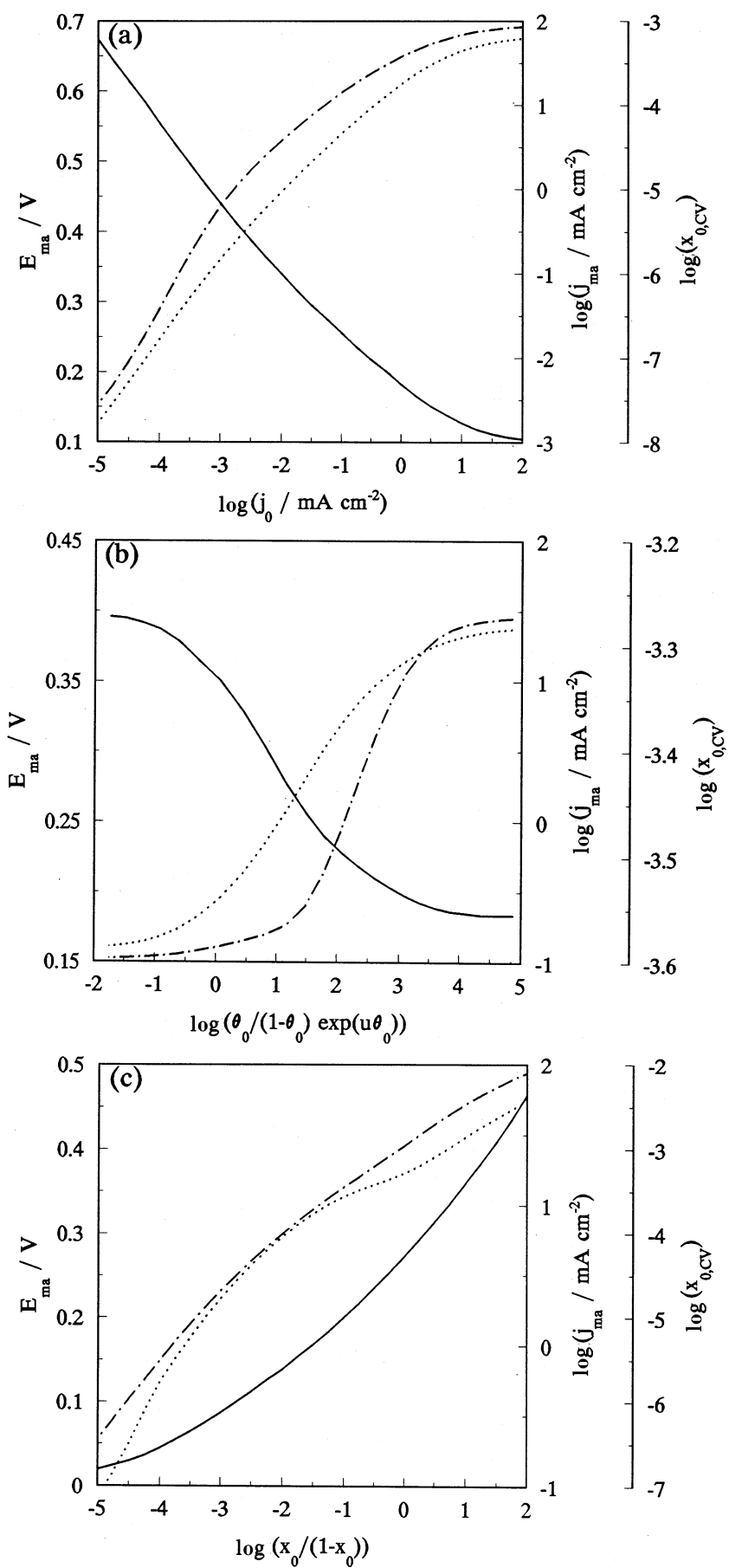


Fig. 2. (Continued)

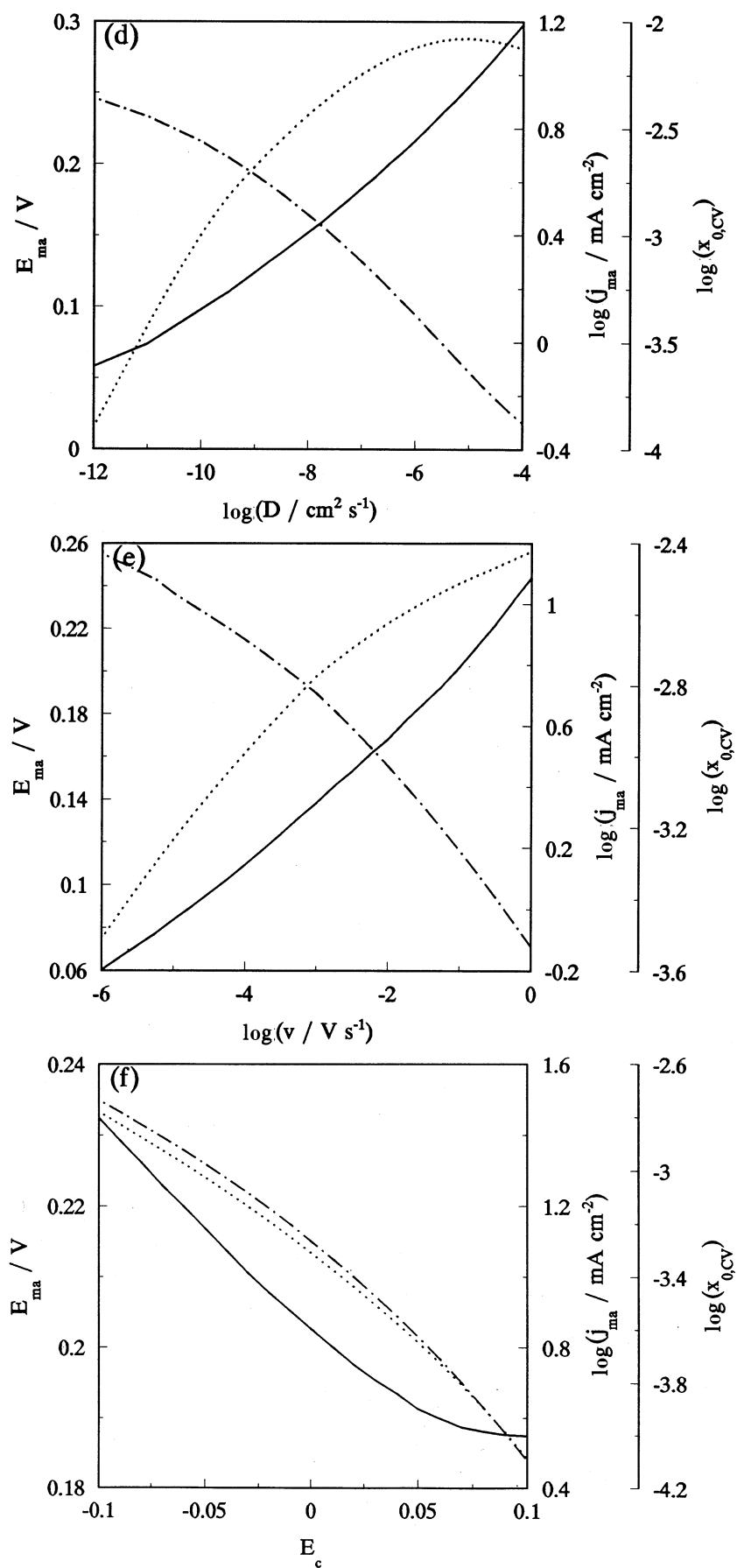


Fig. 2. (Continued)

### 3.3. Effects of various parameters

Although the surface and bulk parameters are fixed for a specific Pd|H system, we extend our discussions to general Pd alloy|H (D) systems, where the surface properties may be affected by additives and pH values etc., and bulk properties may be affected by the alloy components and hydrogen isotopes. Effects of different parameters on the kinetics are illustrated in Fig. 2.

Fig. 2(a) shows the effects of the exchange current density of the Volmer step,  $j_{0V}$ . It is easy to understand that  $E_{ma}$ ,  $j_{ma}$  and  $x_{0,CV}$  approach limiting values when  $j_{0V}$  is high enough ( $10^2 \text{ mA cm}^{-2}$  in Fig. 2(a)), the limiting situations corresponding to the classical reversible diffusion CV results. The surface process (Volmer step) is at pseudoequilibrium and diffusion becomes the rds. Otherwise, when  $j_{0V}$  is very low, the slope  $\partial E_{ma}/\partial \log j_{0V} = -118 \text{ mV decade}^{-1}$  as indicated in Eq. (14). Because  $x_{0,CV}$  changes with  $j_{0V}$ , the change of  $j_{ma}$  with  $j_{0V}$  cannot be predicted as above and we find  $\partial \log j_{ma}/\partial \log j_{0V} \approx 1$  from Fig. 2(a).

The effects of the equilibrium surface coverage  $\theta_0$  display the interplay between the surface and bulk processes (Fig. 2(b)). When  $\theta_0$  is very low, the Volmer step becomes the rds of the overall reaction and the voltammogram corresponds to the classical irreversible diffusion process; Conversely, it becomes a diffusion-controlled process when  $\theta_0$  approaches 1. The middle areas of  $\theta_0$  are for the process under mixed control.

The effects of the heterogeneity factor  $u$  are similar to that of  $\theta_0$  but its influence is less (not shown here).

The influence of the equilibrium loading ratio  $x_0$  and non-ideal interaction factor  $u_b$  is in contrast to this of the surface parameters  $\theta_0$  and  $u$ , the effect of the former is illustrated in Fig. 2(c). When  $x_0$  is low, the diffusion current decreases and the Volmer step becomes the fast step, the CV result approaching the reversible one. But when  $x_0$  is progressively lower ( $x_0 < 10^{-3.5}$  in Fig. 2(c)), the contribution of bulk H atoms in the cd will be less than that of surface ones. The desorption peak shifts towards the lower potential and its shape reduces to a shoulder on the left of the de-adsorption peak till it disappears finally (not shown here). The case of higher  $x_0$  is not considered further as it is unrealistic from the point of view of physics.

Fig. 2(d) shows the effects of the diffusion coefficient  $D$ . When it is high, the slope  $\partial E_{ma}/\partial \log D = 59 \text{ mV decade}^{-1}$  as indicated in Eq. (14); when it is low, the Volmer step becomes reversible and the voltammogram is similar to the case of small  $x_0$  or a thin Pd plate, although  $x_{0,CV}$  is very large at the same time.

Experimental parameters also affect the CV result. Fig. 2(e) shows the effects of the sweep rate  $v$ ; it has similar effects as those of  $D$  when it is high as implied in Eqs. (13) and (14). But when it is low, the case is different: when  $v$  decreases, the diffusion process (proportional to

$v^{1/2}$ ) is more rapid than the Volmer step (proportional to  $v$ ) and the irreversibility is enhanced.

The increment of  $E_c$  results in a decrease of  $x_{0,CV}$  and diffusion becomes reversible,  $E_{ma}$  approaches a constant and  $j_{ma}$ ,  $x_{0,CV}$  decrease correspondingly (Fig. 2(f)).  $E_{ma}$  is independent of  $E_a$ , when  $E_a$  is above  $E_{ma}$ ,  $j_{ma}$  and  $x_{0,CV}$  decrease with increment of  $E_a$  but the influence is less than that of  $E_c$  (not shown here).

## 4. Comparison with experimental results and discussions

We compare the present treatment with the results of an experiment [16] as illustrated in Fig. 3. In the experiment, the reference electrode was Hg|Hg<sub>2</sub>SO<sub>4</sub> sat. K<sub>2</sub>SO<sub>4</sub> (MSE), which has a potential of 0.64 V vs. SHE. We obtain easily that  $E = 0.05\text{--}0.75 \text{ V vs. RHE}$  for pH = 12, and  $E = 0.1\text{--}0.7 \text{ V vs. RHE}$  for pH = 1. Because  $E_* > E_{\beta z} \approx 0.06 \text{ V vs. RHE}$  [30], it is concluded that PdH<sub>x</sub> is in the  $\alpha$ -phase based on the discussion of Section 3.1. We can use the present model to coincide with the results as shown in Fig. 3; we find the coincidence for pH = 1 is very good, but there is some discrepancy for pH = 12, the reason being that the oxide formation region overlaps with the hydrogen region in alkaline solutions [16,21] and causes the interpretation of process for the Pd|H electrode to become complex. It must be pointed out that only the strong H adsorption ( $\theta_0 = 0.64$  for pH = 12 and  $\theta_0 = 0.77$  for pH = 1) can be adopted and give results in agreement, weak adsorption ( $\theta_0 < 1/2$ ) cannot be applied even of qualitatively. The conclusion of the key role of strong H adsorption at the anodic overpotential is not a special case; it is suitable for other experimental results [17–23] as well.

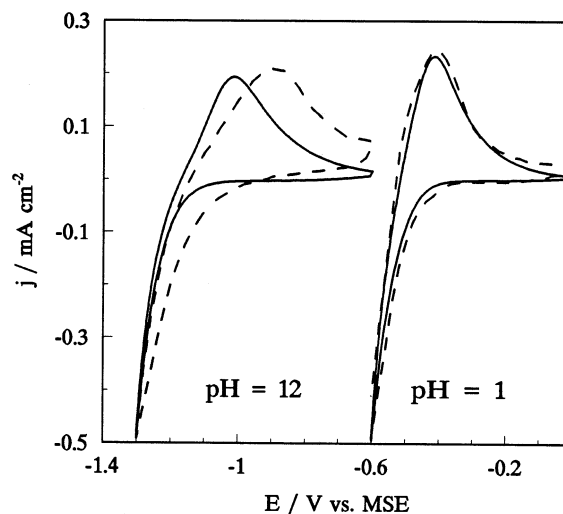


Fig. 3. Comparison of the numerical results (—) with that of the experiment (---), figure 1 in Ref. [16]. Parameters:  $j_{0V} = 0.0425 \text{ mA cm}^{-2}$ ,  $\theta_0 = 0.64$  and  $u = 6.3$  for pH = 12;  $j_{0V} = 0.07 \text{ mA cm}^{-2}$ ,  $\theta_0 = 0.77$  and  $u = 6.6$  for pH = 1; the same parameters are:  $r = 2$ ,  $v = 0.05 \text{ V s}^{-1}$ ,  $j_{0P} = 50 \text{ mA cm}^{-2}$ ,  $x_0 = 0.07834$ ,  $u_b = 0$ ,  $d = 1.25 \times 10^{-3} \text{ cm}$  and  $D = 3.8 \times 10^{-7} \text{ cm}^2 \text{ s}^{-1}$ .

The discussion about the example of CV (Fig. 1) in Section 3 is for strong H adsorption, so it is suitable for the practical situations.

The earlier paper [1] and other bibliographies [24,32] all indicated that  $\theta_0 \ll 1/2$  in charging of H into Pd in the her, but present results show that  $\theta_0 > 1/2$ . The difference is explained only in that there are two sorts of H adsorption on Pd which play different roles in different potential regions. When  $E > 0$ , the strong adsorption determines the kinetic process; When  $E < 0$ , this adsorption is saturated and the weak adsorption takes part in the Pd-H process. The double adsorption [33,34] makes the Pd-H kinetic process fast in a wide range of potential regions.

## 5. Conclusions

Based on the relations of surface reactions developed in the earlier paper [1] and the bulk diffusion equation, we discuss the kinetics of the thick plate Pd|H electrode in cyclic voltammetry. The kinetics must be described by the surface and bulk processes at the same time: when  $cd < 0$  (absorption) the voltammogram exhibits a surface process character; when  $cd > 0$  (desorption) it manifests as diffusion-controlled, but the peak potential displays a mixed control of surface and bulk processes together [22]. On the other hand, the bulk hydrogen concentration in the Pd plate is much less than the equilibrium value. Different Pd–H interaction parameters and experimental factors can affect the kinetics: strong and reversible adsorption of H on Pd, low values of the equilibrium concentration (loading ratio) and diffusion coefficient of H in Pd, fast sweep rate and high  $E_c$  assist with the bulk diffusion being the rds in the kinetics of the  $\alpha$ -PdH<sub>x</sub> electrode.

We give a simple criterion that can judge the existence of phases occurring during CV from the voltammogram. If the potential  $E|_j = 0$  in the positive scan is greater than  $E_{\beta\alpha}$ , the potential for  $\beta\alpha$  phase transition, only the  $\alpha$ -phase is found. Otherwise, the  $\beta$ -phase will be formed in CV.

By comparison with the previous experimental results [16], we find that only strong adsorption can explain the CV results of the  $\alpha$ -PdH<sub>x</sub> electrode. Referring to Ref. [1] and other bibliographies [24,32], we reach a conclusion that H absorption into Pd is controlled by different adsorption at different potentials, i.e. the weak adsorption at  $E$  vs. RHE  $< 0$ , and strong adsorption at  $E$  vs. RHE  $> 0$  are the rds of H absorption into Pd respectively.

## Acknowledgements

The work is supported by the Natural Science Foundation of China and the Foundation of China Academy

of Engineering Physics. We are grateful to Professor Li Bo-Zang for support and Dr Zhang Guang-Cai for helpful discussions.

## References

- [1] W.S. Zhang, X.W. Zhang, H.Q. Li, J. Electroanal. Chem. 434 (1997) 31.
- [2] B.E. Conway, G. Jerkiewicz, J. Electroanal. Chem. 357 (1993) 47.
- [3] Y. Sakamoto, N. Ishimaru, Z. Phys. Chem. (N.F.) 183 (1994) S-311.
- [4] Y. Sakamoto, N. Ishimaru, M. Hasebe, Z. Phys. Chem. (N.F.) 183 (1994) S-319.
- [5] D. Cravens, in: T.O. Passell, M.C.H. McKubre (Eds.), Proc. 4th Int. Conf. on Cold Fusion, vol. 2. Calorimetry and Materials Papers, December 6–9, 1993, Lahaina, Maui, HI, Electric Power Research Institute, Palo Alto, CA, 1994, p. 18–1.
- [6] E. Storms, Fusion Technol. 29 (1996) 261.
- [7] M. Fleischmann, S. Pons, M. Hawkins, J. Electroanal. Chem. 261 (1989) 301, Errata. J. Electroanal. Chem. 263 (1989) 187.
- [8] J. Jorne, J. Electrochem. Soc. 137 (1990) 369.
- [9] S. Szpak, C.J. Gabriel, J.J. Smith, R.J. Nowak, J. Electroanal. Chem. 309 (1991) 273.
- [10] S. Szpak, P.A. Mosier-Boss, C.J. Gabriel, J.J. Smith, J. Electroanal. Chem. 365 (1994) 275.
- [11] A. De Ninno, V. Violante, Fusion Technol. 26 (1994) 1304.
- [12] J.S. Chen, J.-P. Diard, R. Durand, C. Montella, J. Electroanal. Chem. 406 (1996) 1.
- [13] C. Lim, S.-I. Pyun, Electrochim. Acta 38 (1993) 2645.
- [14] C. Lim, S.-I. Pyun, Electrochim. Acta 39 (1994) 363.
- [15] T.-H. Yang, S.-I. Pyun, J. Electroanal. Chem. 414 (1996) 127.
- [16] J. Horkans, J. Electroanal. Chem. 209 (1986) 371.
- [17] J. McBreen, J. Electroanal. Chem. 287 (1990) 279.
- [18] A. Czerwinski, R. Marassi, S. Zamponi, J. Electroanal. Chem. 316 (1991) 211.
- [19] A. Czerwinski, R. Marassi, J. Electroanal. Chem. 322 (1992) 373.
- [20] S. Szpak, P.A. Mosier-Boss, S.R. Scharber, J. Electroanal. Chem. 337 (1992) 147.
- [21] M.M. Jaksic, B. Johansen, R. Tunold, Int. J. Hydrogen Energy 18 (1993) 111.
- [22] A.E. Bolzán, J. Electroanal. Chem. 380 (1995) 127.
- [23] R. Woods, Chemisorption at Electrodes, in: A.J. Bard (Ed.), Electroanalytical Chemistry: a Series of Advances, vol. 9, Marcel Dekker, New York, 1976, p. 1.
- [24] M. Enyo, Hydrogen electrode reaction on electrocatalytically active metals, in: B.E. Conway, J.O'M. Bockris, E. Yeager, S.U.M. Khan, R.E. White (Eds.), Kinetics and Mechanism of Electrode Process, vol. 7, Plenum Press, New York, 1983, p. 241.
- [25] A.J. Bard, L.R. Faulkner, Electrochemical Methods: Fundamental and Applications, ch. 12, Wiley, New York, 1980.
- [26] G.A. Attard, A. Bannister, J. Electroanal. Chem. 300 (1991) 467.
- [27] N. Tateishi, K. Yahikozawa, K. Nishimura, M. Suzuki, Y. Iwanaga, M. Watanabe, E. Enami, Y. Matsudo, Y. Takasu, Electrochim. Acta 36 (1991) 1235.
- [28] M.J. Llorca, J.M. Felio, A. Aldaz, J. Clavilier, J. Electroanal. Chem. 351 (1993) 299.
- [29] M. Baldauf, D.M. Kolb, Electrochim. Acta 38 (1993) 2145.
- [30] F.A. Lewis, The Palladium Hydrogen System, Academic Press, London, 1967, p. 31.
- [31] A.J. Bard, L.R. Faulkner, Electrochemical Methods: Fundamental and Applications, Wiley, New York, 1980, p. 222.
- [32] T. Maoka, M. Enyo, Surf. Technol. 8 (1979) 441.
- [33] V. Breger, E. Gileadi, Electrochim. Acta 16 (1971) 177.
- [34] J.F. Lynch, T.B. Flanagan, J. Phys. Chem. 77 (1973) 2628.